

Contribution of glycosaminoglycans to viscoelastic tensile behavior of human ligament

Trevor J. Lujan,¹ Clayton J. Underwood,¹ Nathan T. Jacobs,¹ and Jeffrey A. Weiss^{1,2}

¹Department of Bioengineering and ²Department of Orthopaedics, University of Utah, Salt Lake City, Utah

Submitted 10 June 2008; accepted in final form 9 December 2008

Lujan TJ, Underwood CJ, Jacobs NT, Weiss JA. Contribution of glycosaminoglycans to viscoelastic tensile behavior of human ligament. *J Appl Physiol* 106: 423–431, 2009. First published December 12, 2008; doi:10.1152/jappphysiol.90748.2008.—The viscoelastic properties of human ligament potentially guard against structural failure, yet the microstructural origins of these transient behaviors are unknown. Glycosaminoglycans (GAGs) are widely suspected to affect ligament viscoelasticity by forming molecular bridges between neighboring collagen fibrils. This study investigated whether GAGs directly affect viscoelastic material behavior in human medial collateral ligament (MCL) by using nondestructive tensile tests before and after degradation of GAGs with chondroitinase ABC (ChABC). Control and ChABC treatment (83% GAG removal) produced similar alterations to ligament viscoelasticity. This finding was consistent at different levels of collagen fiber stretch and tissue hydration. On average, stress relaxation increased after incubation by 2.2% (control) and 2.1% (ChABC), dynamic modulus increased after incubation by 3.6% (control) and 3.8% (ChABC), and phase shift increased after incubation by 8.5% (control) and 8.4% (ChABC). The changes in viscoelastic behavior after treatment were significantly more pronounced at lower clamp-to-clamp strain levels. A 10% difference in the water content of tested specimens had minor influence on ligament viscoelastic properties. The major finding of this study is that mechanical interactions between collagen fibrils and GAGs are unrelated to tissue-level viscoelastic mechanics in mature human MCL. These findings narrow the possible number of extracellular matrix molecules that have a direct contribution to ligament viscoelasticity.

decorin; dermatan sulfate; material properties; tendon; polyethylene glycol

WHEN LIGAMENT IS DEFORMED, temporal molecular realignments induce viscoelastic behaviors. For instance, ligament stiffness will increase at greater strain rates (3, 37) and ligament stresses will dissipate during cyclic loading (36). These well-defined transient behaviors may preserve the structural integrity of ligament by braking excessive joint loads and inhibiting fatigue failure (62). Although functionally significant, the microstructural genesis of ligament's time-dependent behavior is unknown. The identification of molecular interactions that specifically influence tissue-scale viscoelasticity could improve the innovation and evaluation of ligament treatment modalities (e.g., tissue engineering, drug therapy).

The origins of ligament viscoelastic behavior are certainly related to its organization and composition. Ligament can be described as a hydrated (~70% water) fiber-reinforced matrix, in which collagen fibers provide structural integrity to the ground substance matrix. Collagen fibers are formed by arrays of fibrils that in turn are composed of aggregating tropocolla-

gen monomers. These tropocollagen units are tightly wound type I collagen helices, which represent 70% of ligament's solid-phase weight (2). The remaining constituents include other collagens (III, V, X, XII, and XIV), extracellular matrix proteins, and proteoglycans. General theories on the viscoelastic origin in ligament and tendon include inherent viscoelasticity of the collagen fibers (34, 40, 48), interaction of collagen fibers with the extracellular constituents (51), and fluid movement through the solid phase (27, 60). One specific theory that has received considerable attention concerns the interaction between collagen fibrils and sulfated glycosaminoglycans (sGAGs) (9, 11, 40, 44).

sGAGs are negatively charged polysaccharide macromolecules that covalently attach to proteoglycan core proteins. The sGAGs in ligament include dermatan sulfate, chondroitin sulfate (A and C), and keratan sulfate. Dermatan and chondroitin sulfate make up the majority of all sGAGs in ligament and are the exclusive sGAG chains of the interfibrillar proteoglycans biglycan and decorin. Biglycan attaches to collagen fibrils through its sGAG chains (38), while decorin, which represents ~90% of all ligament proteoglycans (22), attaches to collagen fibrils through the regular binding of its core protein on D-period sites (53). The sGAG chains of biglycan and decorin span fibrils (42, 53) and are preferentially distributed orthogonal to the fibril direction (19). Since sGAGs have been shown to self-associate (28), interactions between sGAGs on neighboring fibrils have the capacity to influence the fibril sliding that is attributed with tensile stretch (40). Although interfibrillar sGAGs are unlikely to influence quasi-static ligament mechanics (31), sGAGs may still resist transient tensile loads (9, 49). Furthermore, sGAGs are highly negatively charged and through collagen fibril interactions create a fixed charge density that influences tissue hydration (26), and potentially viscoelastic behavior (8, 56).

Experimental and theoretical studies have investigated the viscoelastic mechanical influence of sGAGs during tensile deformation. Research by Robinson et al. (47) and Elliott et al. (11) found that, relative to adult wild-type mice, the tensile behavior of tendon tail fascicles in decorin-deficient mice had reduced strain rate sensitivity and faster stress relaxation. These results indicate that sGAGs may be strongly associated with tensile viscoelastic properties in tendon. Furthermore, degradation of sGAGs significantly altered tensile viscoelastic properties in lung parenchymal strips (1) and in bovine cartilage (49). No studies have directly measured the influence of sGAGs in ligament, but theoretical studies did successfully

Address for reprint requests and other correspondence: J. A. Weiss, Dept. of Bioengineering, Univ. of Utah, 50 South Central Campus Dr., Rm. 2480, Salt Lake City, UT 84112 (e-mail: jeff.weiss@utah.edu).

The costs of publication of this article were defrayed in part by the payment of page charges. The article must therefore be hereby marked "advertisement" in accordance with 18 U.S.C. Section 1734 solely to indicate this fact.

predict viscoelastic behavior of tendon by accounting for sGAG-fibril interactions (9, 40).

Collectively, the previous studies have identified sGAGs as macromolecules likely connected to viscoelastic tensile properties in ligament. Yet the mechanical alterations observed in decorin-deficient mice (11, 47) were not specific to sGAGs, and experimental results in parenchymal lung and cartilage tissue may not translate to ligament, where sGAGs are more sparsely distributed (2, 57). Therefore, the aim of this study was to specifically determine whether interfibrillar sGAGs influence the viscoelastic material behavior of ligament under tension. To meet this objective, it was necessary to control for tissue hydration and collagen fiber stretch, which independently impact ligament mechanics (8, 37, 56).

MATERIALS AND METHODS

Summary of experimental design. The medial collateral ligament (MCL) of the human knee was chosen as a model ligament because of a distribution of sGAGs comparable to other knee ligaments (2) and our well-established experimental protocol for mechanical characterization (3, 41). Samples extracted from cadaveric MCLs were subjected to tensile loading along the fiber direction on a material testing system. This configuration best represents the principal loading orientation in ligament (33). After tensile testing was completed, samples were removed from the material testing system and incubated in either a control or chondroitinase ABC (ChABC) treatment. ChABC degrades chondroitin sulfate (types A and C, or chondroitin-4-sulfate and chondroitin-6-sulfate) and dermatan sulfate without affecting other proteoglycan macromolecules (17, 63) and has been reported to remove at least 88% of interfibrillar sGAGs (31). Mechanical testing was then repeated on each specimen to determine the treatment effect. To measure whether this treatment effect was influenced by testing parameters, strain level and buffer solution were varied to make eight groups, with $n = 5$ samples in each group, for a total of 40 samples.

Viscoelastic testing. Eleven unpaired human MCLs were used for this experiment [donor age = 54 yr (SD 10)]. Six MCLs were used for viscoelastic testing at a 4% strain level, and five MCLs were used for viscoelastic testing at a 6% strain level. Knees were acquired fresh-frozen and were allowed 16 h to thaw before dissection. Knees with ligament lacerations, surgical scars, or cartilage wear characteristic of osteoarthritis were eliminated. During dissection, the tissue was kept moist by application of a physiological 0.9% saline buffer solution through a nozzle. A hardened steel punch was used to extract four tensile samples from different locations in each superficial MCL between the tibial and femoral insertions (Fig. 1A) (41). Two strips of tissue immediately adjacent to the punched tensile sample were retained to monitor tissue hydration in an unloaded state (Fig. 1B). The punch shape included beveled ends for gripping and was oriented so that its long axis was aligned with visible fiber bundles. Two black optical markers were adhered with cyanoacrylate to the narrow central third of the tensile samples. Samples were loaded in the clamping assembly (31, 32), and width and thickness dimensions were determined by taking an average of three measurements with digital calipers (Mitutoyo, San Jose, CA; accuracy ± 0.02 mm).

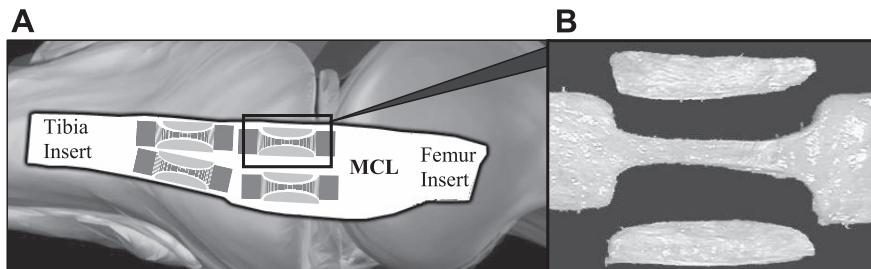
Mechanical testing was performed in a custom-built testing chamber that interfaced with a heating recirculator (PolyScience, Niles, IL; accuracy $\pm 0.2^\circ\text{C}$) to maintain a solution temperature of 37°C (18, 36).

The testing protocol consisted of preconditioning followed by a recovery period and then dynamic loading (Fig. 2). To establish a consistent reference position for all samples, a 0.1-N preload was applied (Sensotec, Columbus, OH; max range 29 N, accuracy ± 0.03 N). At this reference position, clamp-to-clamp specimen length was determined by averaging three measurements taken with an inside caliper (Mitutoyo; accuracy ± 0.02 mm). To precondition the samples, the tissue was lengthened by 8% at a strain rate of 1%/s and held for 5 min before being returned to its reference position. Next, a triangular displacement profile stretched the tissue by 8% for 10 cycles at a strain rate of 1%/s. The 8% strain amplitude was selected to exceed the highest strain level experienced during the testing protocol (55), while not damaging the tissue (31, 39). Since sGAGs should not influence quasi-static ligament mechanics (31), peak stresses during the final pre- and posttreatment preconditioning cycles were compared to verify that the extended test procedure did not cause unexpected damage to the tissue (Fig. 2).

After preconditioning, samples were returned to their reference length and allowed 10 min to recover. Specimens were then ramped at 1%/s to a prescribed strain level of 4% or 6% clamp-to-clamp strain and allowed to stress-relax for 10 min (Fig. 2). At a 4% strain level, the stress-strain response is still in the toe region (31) and the collagen fibers are not completely uncrimped (4). At a 6% strain, the stress-strain response is in the linear region and the collagen fibers are collectively straightened (4, 15). Testing these two strain levels permitted the assessment of sGAGs at different states of collagen and ground substance contribution. After stress relaxation, sinusoidal displacement waves were applied for 10 cycles at each frequency (0.1, 1, 5, 10, and 15 Hz) to an amplitude of 0.125% clamp-to-clamp strain (Fig. 2). The 15-Hz sinusoidal oscillation corresponds to a maximum strain rate of $\sim 12\%/s$. The tissue strain [roughly 50% of the clamp-to-clamp strain (31)] was measured with a validated optical tracking system (29). This system recorded at 30 Hz; therefore the tissue strain during 0.1-Hz oscillations was used to predict the tissue strain for all sinusoidal frequencies (3). There was an average drop of 0.6% (SD 0.4) in the equilibrium stress level between the start and completion of the entire set of oscillations. This small drop verified that 10 min of stress relaxation was sufficient for equilibrium to be reached.

After completion of the test protocol, each sample was removed from the material testing system while still mounted in the clamps. The entire specimen and clamp assembly was bathed for 1 h at room temperature in the buffer solution (detailed below) with protease inhibitors (1 tablet of mini-Complete per 10 ml of buffer). This was followed by 6 h of incubation in the buffer solution with or without ChABC treatment (1.0 IU/ml, Sigma-Aldrich, Buchs, Switzerland). The specimen was unloaded during the entire incubation phase. After incubation, the clamp assembly was reattached to the material testing system and returned to the original testing position. Mechanical tests were then repeated with parameters identical to the pretreatment mechanical tests. The spatial reproducibility of the clamping assembly

Fig. 1. A: illustration of specimen acquisition. Up to 4 specimen sets were extracted from each medial collateral ligament (MCL), with 3 samples to each set. Each set included 1 punched sample for viscoelastic tensile testing (dark gray) and 2 adjacent strips to monitor tissue hydration (light gray). B: photograph of the specimen set.



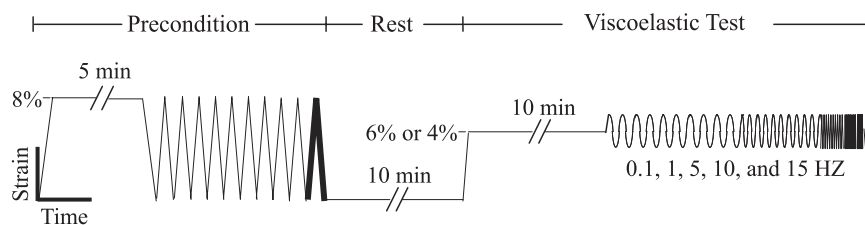


Fig. 2. Viscoelastic protocol (clamp-to-clamp strain as a function of time). After preloading to 0.1 N, specimens were preconditioned. Peak stress was analyzed from the 10th preconditioning cycle (bold). Specimens were allowed to recover for 10 min before stress relaxation and sinusoidal displacements (amplitude = 0.125% strain).

and treatment protocol are described to greater detail in our previous publication (31).

Tissue swelling. To control tissue swelling, two testing solutions were used throughout the experiment. One solution consisted of a physiological buffer mixture (15 ml of 20 mM Tris pH 7.5, 150 mM NaCl, 5 mM CaCl₂) and was designated the standard buffer. A second solution was this buffer plus 7.5% polyethylene glycol (PEG, 10 kDa; Fluka, Buchs, Switzerland) and was designated the PEG buffer. Solutions containing PEG and sodium chloride have been used to control swelling in metabolically inactive tissue (7, 10, 21, 45), and this concentration has been shown to maintain wet weight in ligament during prolonged immersion (32). Samples were equilibrated in their respective buffer solutions for at least 2 h before pretreatment mechanical tests. All mechanical tests and incubations were performed in their respective buffer solutions.

Multiple techniques were employed to quantify tissue swelling during the course of the experiment. Adjacent to each tensile sample, two strips were harvested to monitor tissue hydration (Fig. 1B). One strip was weighed and immediately frozen to serve as the *time 0* control for water content. The second strip shadowed the testing protocol of the mechanically tested specimen in an unloaded state. For example, this sample was immersed in solution from the testing chamber during mechanical tests and was included in the same incubation compartment as the mechanically tested sample. It was therefore possible to assess whether the wet weight of the tissue had been altered during mechanical testing and incubation. After the posttreatment mechanical tests, tensile samples were excised from the clamps. Tensile samples and their adjacent strips were then weighed, rinsed, frozen, and lyophilized. Water content was calculated from the ratio of dry weight to final wet weight (APX-60, Denver Instruments, Denver; readability ± 0.1 mg).

Verification of sGAG removal. The efficacy of the ChABC treatment was determined by using dimethylmethylene blue assays to measure the concentration of sGAGs in papain-digested samples before and after retreatment with ChABC (1, 31). The percentage of degraded sGAGs in ChABC-incubated samples was estimated by subtracting the amount of sGAGs (μg sGAG/mg dry wt) in the papain-digested sample from the sGAGs in the same sample after additional ChABC treatment. This value, which represents the amount of sGAGs undigested during incubation, was normalized to the native sGAG concentration. Native sGAG estimates were calculated by averaging the amount of sGAGs in all the *time 0* control specimens. Since ChABC does not degrade keratin or heparin sulfate, this native sGAG estimate was first reduced by the amount of sGAGs in the *time 0* control after ChABC treatment. An approximation of the efficacy of ChABC could thus be attained, along with the percentage of sGAGs that could not be degraded by ChABC.

Data reduction and statistical analysis. To generate stress-strain curves, the first Piola-Kirchhoff stress was determined with tissue strain data from the optical tracking system [$(l - l_0)/l_0$, where l is the current length and l_0 is the reference length] (29). The stress-time curves from the stress relaxation tests were normalized by the peak stress to obtain reduced relaxation curves (13). The cyclic strain-time and stress-time data from the final four cycles of each frequency were fit to a four-parameter sine function in Matlab:

$$y = y_0 + A \sin\left(\frac{2\pi t}{b} + \phi\right) \quad (1)$$

Here, y and t represent the strain (or stress) and time data, respectively, y_0 represents the equilibrium strain (or stress) level, and A denotes the amplitude of the sine wave; ϕ represents the phase, and b denotes the inverse of the frequency (1/Hz). The data (y, t) from the final four cycles were used to fit the four unknown parameters [average $r^2 = 0.998$ (SD 0.002)]. Substituting data (y, t) from the final two cycles did not significantly alter the parameter values (data not shown). Dynamic modulus M (MPa) and phase shift ϕ (radians) were calculated for all frequencies:

$$M = \frac{A_\sigma}{A_\epsilon}; \quad \phi = \phi_\sigma - \phi_\epsilon \quad (2)$$

A_σ and A_ϵ denote amplitudes of the cyclic stress-time and strain-time data, respectively, while ϕ_σ and ϕ_ϵ denote the corresponding phase angles (12).

Statistical analysis was performed in several parts. First, the effect of incubation on each of the eight groups' material properties was assessed by using paired *t*-tests with data taken at two time points (pre- and posttreatment, sample size of 5 for each group). Second, the overall effects of treatment, buffer solution, and strain level on mechanical properties were assessed with analysis of covariance (ANCOVA), by controlling for pretreatment results. This analysis included data from all 8 groups; therefore the total sample size for each comparison (e.g., ChABC vs. control) was 40. All pairwise comparisons were made with Bonferroni adjustments. The effect of frequency on dynamic modulus and phase shift was evaluated with repeated-measures ANOVA (within-subject factors: frequency and time). Finally, biochemistry results were determined by using independent *t*-tests to measure treatment effect on sGAG content. A priori, the sample size was selected to detect with 80% confidence (Power = 0.80) a 10% change in mechanical properties due to treatment and a 20% change in mechanical properties due to other independent variables. A posteriori, confidence intervals were used for equivalence testing (50). Significance was set to $P \leq 0.05$, and all results are reported with standard deviation unless otherwise noted.

RESULTS

Reduced relaxation data. The reduced relaxation curves were unaffected by incubation for all combinations of treatments, buffer solutions, and strain levels (Fig. 3, Table 1). The percent relaxation for all tests was 30.0% (SD 4.9) before incubation and 30.6% (SD 5.2) after incubation. The percent relaxation of all samples tested at the lower strain level, 31.8% (SD 4.2), was significantly greater than that at the higher strain level, 28.1% (SD 5.0) ($P = 0.01$). After incubation, the percent increase in percent relaxation varied by 0.2% due to treatment ($P = 0.69$), 3.2% due to buffer solution ($P = 0.41$, greater increase with PEG buffer), and 4.1% due to strain level ($P = 0.02$, greater increase at 4% strain level). At a 95% confidence level, values for the difference in percent relaxation due to

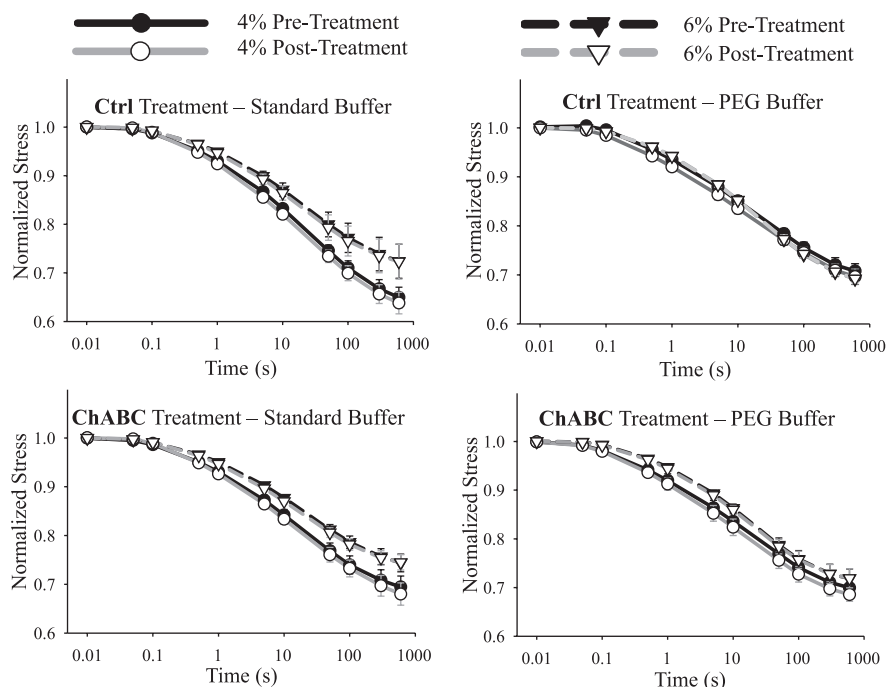


Fig. 3. Reduced relaxation curves for control-treated specimens in either standard buffer (top left) or polyethylene glycol (PEG) buffer (top right) and chondroitinase ABC (ChABC)-treated specimens in either standard buffer (bottom left) or PEG buffer (bottom right). Keys indicate applied clamp-to-clamp strain for pre- and posttreatment results. Values are means ± SE.

treatment ranged between -1.1% and +1.6%. Therefore, there is 95% confidence that ChABC had a <5.4% effect on reduced relaxation.

Dynamic modulus. The average dynamic modulus (averaged over all frequencies) was significantly increased by incubation in two of the eight test groups by 4.4% (SD 3.0) (Fig. 4, Table 1). The average dynamic modulus for all specimens at 0.1 Hz was 424 MPa (SD 304) before incubation and 434 MPa (SD 318) after incubation, while at 15 Hz it was 501 MPa (SD 350) before incubation and 522 MPa (SD 373) after incubation. The samples tested at the higher strain level had a dynamic modulus 226% greater than the lower strain level ($P < 0.001$). Oscillation frequency only had a significant effect on dynamic modulus for the two test groups control treated in standard buffer, which corresponds to the groups with the lowest standard deviations. After incubation, the percent increase in the dynamic modulus varied by 0.3% due to treatment ($P = 0.86$), 0.1% due to buffer solution ($P = 0.96$), and 4.2% due to strain

level ($P = 0.20$, greater increase at 6% strain level). At a 95% confidence level, values for the difference in dynamic modulus due to treatment ranged between -17 and +20 MPa. Therefore, there is 95% confidence that ChABC had a <4.3% effect on dynamic modulus.

Phase shift. The average phase shift (averaged over all frequencies) was significantly increased after incubation in four of the eight test groups by 9.5% (SD 6.7) (Fig. 5, Table 1). The average phase shift for all specimens at 0.1 Hz was 0.062 rad (SD 0.027) before incubation and 0.069 rad (SD 0.025) after incubation, while at 15 Hz it was 0.155 rad (SD 0.025) before incubation and 0.169 rad (SD 0.034) after incubation. The average phase shift at the 4% strain level, 0.114 rad (SD 0.019), was significantly greater than that at the 6% strain level, 0.095 rad (SD 0.008) ($P < 0.001$). Oscillation frequency significantly affected phase shift for all groups. After incubation, the percent increase in phase shift varied by 0.1% due to treatment ($P = 0.98$), 5.2% due to buffer solution ($P = 0.32$,

Table 1. Mechanical properties before and after treatment

	4% Strain Level						6% Strain Level					
	Standard buffer			PEG buffer			Standard buffer			PEG buffer		
	Pretreat	Posttreat	SE	Pretreat	Posttreat	SE	Pretreat	Posttreat	SE	Pretreat	Posttreat	SE
Control treated												
Avg. peak stress, MPa	5.3	5.4	0.1	5.5	5.8	0.1	6.8	6.7	0.1	9.6	9.9	0.2
Avg. stress relax, %	36.1	36.6	0.9	29.4	31.1	1.0	28.1	28.4	0.3	31.0	31.2	0.6
Avg. dynamic modulus, MPa	176	181	5	264	280	9	485	501	2	758	786	12
Avg. phase shift, rad	0.104	0.118	0.004	0.124	0.133	0.004	0.089	0.098	0.002	0.101	0.104	0.002
ChABC treated												
Avg. peak stress, MPa	8.3	8.4	0.1	7.0	7.0	0.1	7.9	7.8	0.1	11.6	11.9	0.1
Avg. stress relax, %	31.6	32.4	0.8	30.0	32.4	1.8	28.0	27.7	0.4	25.4	25.1	0.3
Avg. dynamic modulus, MPa	374	361	25	361	369	10	671	726	23	627	655	7
Avg. phase shift, rad	0.106	0.120	0.006	0.116	0.126	0.002	0.091	0.098	0.003	0.099	0.104	0.001

$n = 5$ samples each for 8 test groups. PEG, polyethylene glycol; ChABC, chondroitinase ABC; SE, standard error of the mean for paired differences. SE values in bold represent statistically significant differences between related pre- and posttreatment mechanical properties ($P < 0.05$).

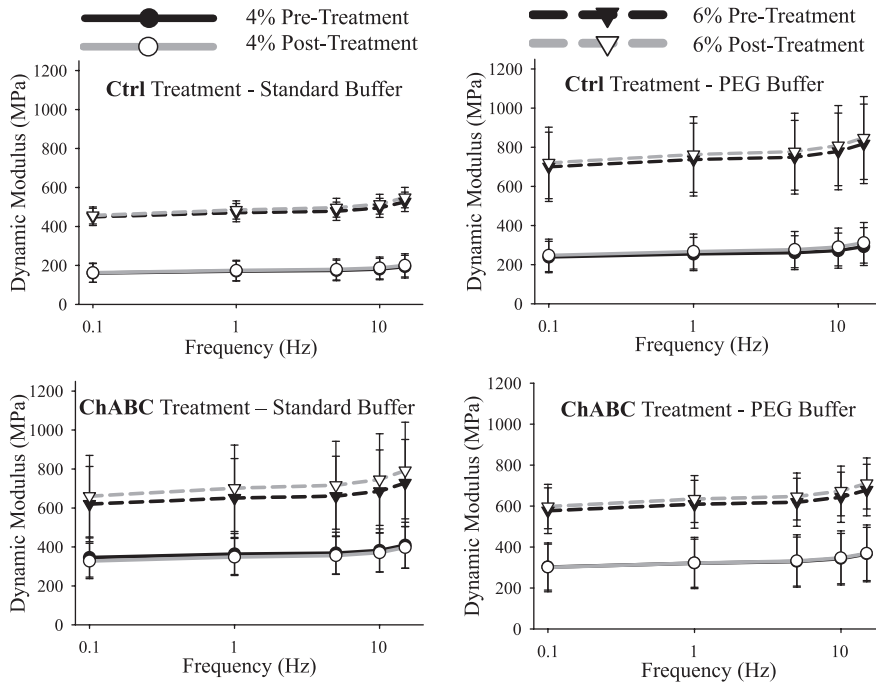


Fig. 4. Dynamic modulus as a function of oscillatory frequency for control-treated specimens in either standard buffer (top left) or PEG buffer (top right) and ChABC-treated specimens in either standard buffer (bottom left) or PEG buffer (bottom right). Keys indicate applied clamp-to-clamp strain for pre- and post-treatment results. Values are means \pm SE.

greater increase in standard buffer), and 5.3% due to strain level ($P = 0.02$, greater increase at 4% strain level). At a 95% confidence level, values for the difference in phase shift due to treatment ranged between -0.005 and $+0.005$ rad. Therefore, there is 95% confidence that ChABC had a $<4.5\%$ effect on phase shift.

Tissue swelling. The average wet weight of unloaded samples increased by 16% (SD 10) when tested in standard buffer and decreased by 11% (SD 5) when tested in PEG buffer (Fig. 6). Unloaded samples tested in standard buffer had a significantly greater wet weight than those tested in PEG buffer ($P <$

0.001). There was no effect of treatment on the overall normalized wet weight ($P = 0.68$). During the incubation period, the average wet weight in the unloaded samples decreased by 1.3% (SD 5.6) ($P = 0.48$) in the standard buffer and increased by 3.9% (SD 7.2) ($P = 0.08$) in the PEG buffer. The greatest change during the incubation period was a 3.7% (SD 6.4) decrease in wet weight in samples treated with ChABC in standard buffer ($P = 0.15$).

The water content of native samples was consistent between treatment and buffer solution groups, with an average range from 71.6% to 73.1% (Fig. 7). All tested samples had water

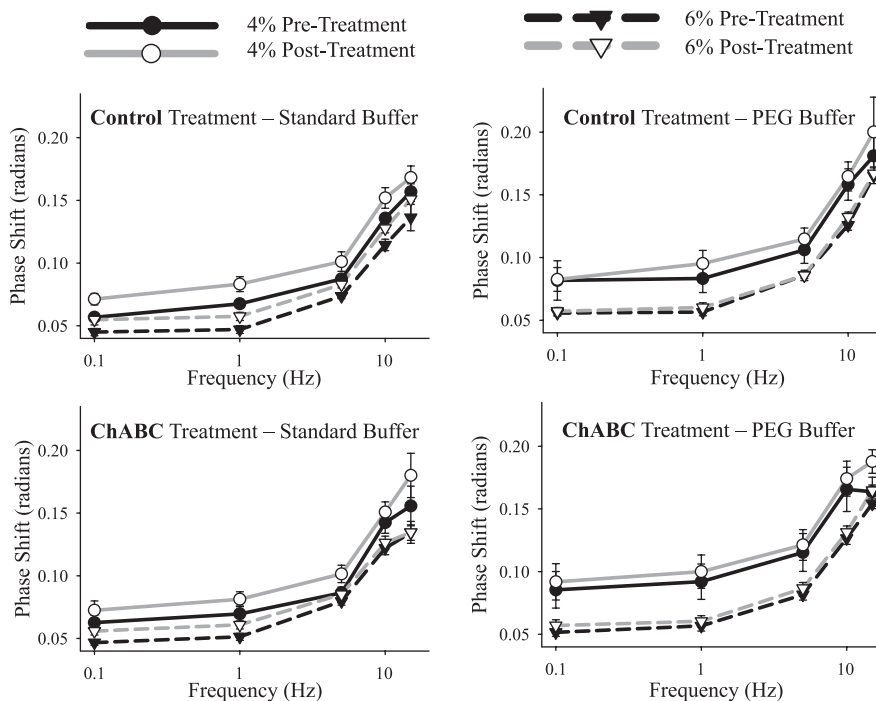


Fig. 5. Phase shift as a function of oscillatory frequency for control-treated specimens in either standard buffer (top left) or PEG buffer (top right) and ChABC-treated specimens in either standard buffer (bottom left) or PEG buffer (bottom right). Keys indicate applied clamp-to-clamp strain for pre- and post-treatment results. Values are means \pm SE.

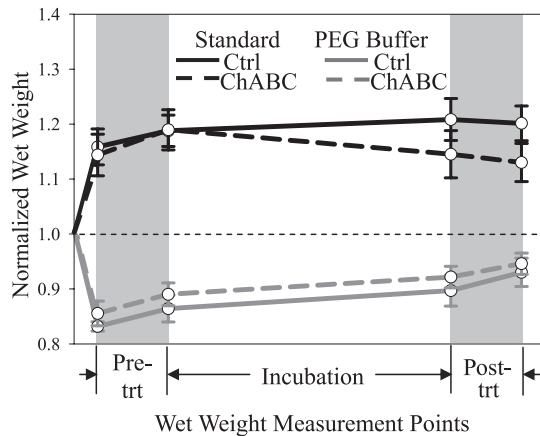


Fig. 6. Time history of the unloaded samples' wet weight through the course of the experiment. Wet weight was normalized to the initial weight of the unloaded sample immediately after dissection. All samples equilibrated in buffer solution for at least 2 h before pretreatment test. The 4% and 6% strain level groups were combined.

content significantly different from that of the native samples, with the exception of the mechanically loaded samples tested in standard buffer (average water content = 72.3, $P = 0.24$). Compared with the native samples, unloaded samples incubated in the PEG buffer had a significantly decreased water content and unloaded samples incubated in standard buffer had a significantly increased water content ($P < 0.001$ and $P < 0.001$, respectively). The mechanically loaded samples had 2.5% less water content than the unloaded samples ($P = 0.002$). Although treatment type and strain level had no significant effect on water content after incubation ($P = 0.29$ and $P = 0.52$, respectively), ChABC-treated samples had 2.2% less water content than control-treated samples when tested in standard buffer.

Experimental reproducibility and efficacy. Reproducibility of the pretreatment mechanical tests was confirmed by optically measuring posttreatment clamp positions to be within 0.04 mm (SD 0.02) of the pretreatment clamp positions. For all treatments, buffer solutions, and strain level combinations, incubation affected the average peak stress by <5% (Table 1). One group did experience a significant increase in peak stress after incubation (Table 1), but by only 2.7% (SD 1.7) ($P = 0.03$). A qualitative comparison verified that the 4% and 6% clamp-to-clamp strains were indeed in the toe and linear stress-strain regions, respectively (data not shown).

The ability of ChABC digestion of sGAGs was dependent on the buffer solution. ChABC treatment of the *time 0* reference samples removed 90% (SD 6) of sGAGs. The *time 0* reference samples in the standard and PEG buffer groups had 4.2 (SD 1.9) and 4.4 (SD 2.2) μg sGAG/mg dry tissue, respectively. Samples that were mechanically tested in the standard buffer and treated with ChABC had an average of 0.7 μg sGAG/mg dry tissue at the end of testing, an 83% reduction in sGAG content (92.6% treatment efficacy). Samples that were mechanically tested in the PEG buffer and treated with ChABC had an average of 1.6 μg sGAG/mg dry tissue at the end of testing, a 64% reduction in sGAG content (70.0% treatment efficacy). The sGAG reduction in mechanically tested samples treated with ChABC was significantly less in the PEG buffer compared

with the standard buffer ($P = 0.03$). The native samples had on average 20% more sGAGs than the unloaded samples that endured the entire testing protocol ($P = 0.23$).

DISCUSSION

The aim of this research was to determine the specific influence of interfibrillar sGAGs on ligament viscoelasticity. Viscoelastic properties were measured before and after incubation in either control or ChABC treatment. Although the incubation process moderately increased dynamic modulus and phase shift, these moderate increases were independent of treatment (control or ChABC). At a 95% confidence level, ChABC had a <5.4% effect on any measured viscoelastic property. Therefore, this study found no biologically significant relationship between fibril-sGAG mechanical interactions and tissue-level viscoelasticity in human MCL.

The primary function of ligament is to resist tensile loads. It is becoming clear that interfibrillar sGAGs do not directly support the quasi-static (31) and viscoelastic mechanisms required to support this function. In cartilage, however, sGAGs were found to moderately control the kinetics of the viscoelastic response through sGAG-collagen interactions (25, 4964). Therefore, sGAGs appear to have different functional roles in ligament and cartilage. This may be due to the low concentrations of sGAGs in ligament (<1% dry wt) relative to cartilage (15–30% dry wt) and the differences in anisotropy and collagen organization. Our findings also diverge from a study reporting that sGAG removal increases hysteresis in parenchymal lung tissue (1). Compositional and structural differences between ligament and lung tissue may again account for the conflicting results. Additionally, the parenchymal lung study was unable to reproduce material properties in the control group with a repeated-measures experimental design, which complicates the interpretation of their findings. It is emphasized that the results of the present study are only applicable to tensile loads. It is possible that sGAGs physically resist compression in mature human ligament, since sulfated GAG-fibril networks are known to retard fluid exudation (16) and the location of high sGAG concentrations in ligament coincides with regions that experience high compressive stresses (24).

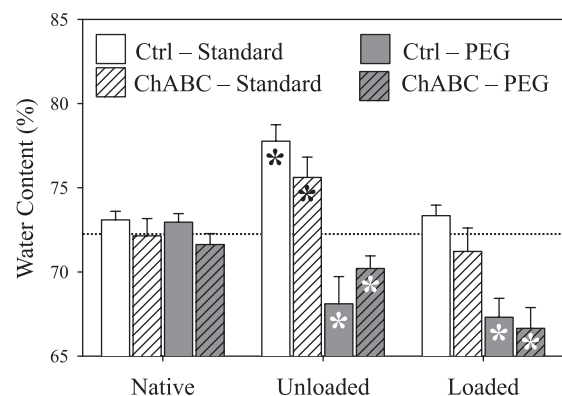


Fig. 7. Water content of the *time 0* reference samples (native), the incubated samples that were not mechanically tested (unloaded), and the incubated samples that were mechanically tested (loaded). The 4% and 6% strain levels were combined. *Significant difference ($P < 0.05$) from the average native water content (horizontal line).

Even though sGAGs do not appear to directly resist tensile loads, they likely have an indirect effect by modulating collagen fibrillogenesis (52, 59). Mouse knockout studies identified decorin as a proteoglycan that influences elastic and viscoelastic tensile behavior in tendon (11, 47). On the basis of the results of the present study, it appears that these mechanical alterations were due to compensatory or developmental abnormalities intrinsic to decorin-deficient mice. For instance, histological studies have shown decorin deficiency to cause irregularly sized and spaced fibrils, which is likely caused by the absence of interfibrillar sGAGs that normally inhibit lateral fibril fusion (43). Although tendon and ligament have unique histological and biochemical characteristics, they also exhibit gross compositional similarities, and ligaments have higher GAG concentrations than tendons (2). Therefore, it is appropriate to extend the results of the present study to tendon.

The mechanical property most impacted by incubation was phase shift. Phase shift, which quantifies energy dissipation, increased by 8.4% in control-treated samples and 8.5% in ChABC samples. Although this increase was only significant in half the tested groups (Table 1), it was observed in 35 of the 40 tested samples. A similar time-dependent effect occurs in articular cartilage. Cartilage tested after control-treated incubation exhibited greater creep (49) and phase shift (64) than cartilage tested immediately on dissection. This effect may tie into the observed relationship between strain level and viscoelastic alterations after incubation. For example, samples tested at the 4% strain level were more apt to dissipate energy after incubation than samples tested at the 6% strain level. This would indicate a time-dependent degradation of structures or networks that provide elastic function at low strain rates, such as elastin (35). Interestingly, during our preliminary studies using the same test procedure (Fig. 2), we observed that phase shift increased by only $1.4 \pm 3.3\%$ after incubation ($n = 4$). The only deviation in the preliminary protocol was that tests were conducted on specimens that had been thawed and refrozen multiple times. Therefore, this *in vitro* loss in energy storage appears to equilibrate with time.

The experimental protocol needed to be sensitive to small alterations in material properties. A repeated-measures design was thus incorporated to reduce the inter- and intraspecimen variability that has been observed mechanically and chemically in ligament (31). To test the reproducibility of the protocol, a quantitative comparison of peak stress values was made to confirm that pretreatment mechanical tests did not damage the sample and cause a reduction in posttreatment mechanical behaviors. Pretreatment and posttreatment peak stress values were indeed verified to be within 5% for all test groups. Several protocol revisions were required to achieve this consistency. The material property values of this study are consistent with previous research that defined the viscoelastic properties of human MCL (3). Variations in phase shift between these studies may be due to different testing environments [fluid chamber vs. humidity chamber (3)]. Since specimens were extracted from four distinct regions in the MCL, the material properties and conclusions of this study are representative of the longitudinal (proximal and distal) and oblique fiber zones of the superficial MCL.

Incubation in ChABC successfully removed the interfibrillar sGAGs chondroitin and dermatan sulfate. In standard buffer, ChABC-treated samples had a 92% reduction of chondroitin

and dermatan sulfates, while in PEG buffer ChABC-treated samples had a 70% reduction in chondroitin and dermatan sulfates. These degradation values are higher than or similar to those reported in other studies that used ChABC in connective tissue (1, 14, 23). Our previous study (31) used transmission electron microscopy imaging with Cupromeronic Blue staining to determine that ChB reduced interfibrillar sGAGs by 88%. Therefore, we are confident that the majority of interfibrillar sGAGs were degraded. The PEG buffer significantly lessened the effectiveness of ChABC, which is likely due to the increased viscosity of the buffer solution and the inverse relationship between viscosity and diffusion (Stokes-Einstein relation). ChABC will also degrade hyaluronic acid (63), a large unsulfated GAG that is noncovalently associated with aggrecan and is chemically similar to chondroitin sulfate. Therefore, this macromolecule does not appear to influence viscoelasticity in human MCL. On the basis of the effectiveness of ChABC in degrading hyaluronic acid (degrades >95% in ligament samples) (58), this macromolecule does not appear to influence viscoelasticity in human MCL. Biochemical assays showed that chondroitin and dermatan sulfate represent 90% of total sGAGs in the MCL samples. The remaining 10% of sGAGs likely includes keratan sulfate and heparin sulfate. These sGAGs may contribute to ligament viscoelasticity, but this is unlikely given their low concentrations and distribution near fibroblasts (5).

Tissue hydration was controlled by immersing samples throughout the entire testing protocol in one of two types of buffer solution. One buffer included 7.5% PEG to create a hypertonic solution that reduced tissue swelling (10, 45). The philosophy behind testing in different buffer solutions was to ensure that our findings were neither dependent on a particular hydration state nor masked by swelling. Preconditioning the samples in each buffer solution helped minimize fluctuations in tissue hydration during testing. Previous research indicated that concentrations of 0.9% saline and 7.5% PEG successfully maintained initial wet weight in ligament, with a 5% decrease in water content (32). In the present study, these same concentrations caused more pronounced tissue dehydration, perhaps due to the addition of calcium chloride (45). Under mechanical loading, this study found standard buffer to best maintain the native water content of ligament.

The negligible effect of hydration on mechanical properties has implications for modeling ligament behavior with biphasic theory. Fluid flow can contribute to viscoelasticity through solid-fluid interactions that result in frictional drag (6). These biphasic interactions are dependent on permeability, which is a function of sGAG concentration and water content (54). Since sGAG extraction and water content fluctuations had no effect on viscoelastic characteristics, fluid flow appears not to contribute to viscoelastic effects in organized structures such as ligament that have low concentrations of sGAGs. Other studies have reached similar conclusions (1, 20). The present study, however, is limited in supporting this statement, for two reasons. First, sulfate groups may have remained in the tissue after being cleaved and continued to influence fluid permeability. Second, fluid flow mechanisms in ligament may be insensitive to 10% fluctuations in gross water content. Future studies that specifically examine fluid flow mechanisms in ligament through experimental or theoretical approaches could better address this postulation.

A principal limitation of this research is that biochemical composition within the ligaments may have been altered post-mortem. This concern is justified by research that found freezing rabbit ligament caused significant changes in hysteresis during tensile tests (36, 61), yet the measured change was small and its relevance has been questioned (36). It is unlikely that the *in vivo* conditions of the MCL were perfectly replicated in this experiment, although every effort was made to provide a physiological testing environment (e.g., temperature, hydration, protease inhibitors). Finally, the prolonged effect of sGAG deprivation was not investigated in this study. Removal of sGAGs may eventually cause fibril abrasion and microstructural damage.

In conclusion, this study demonstrated that mechanical interactions between sGAGs and collagen fibrils are unrelated to tissue-level viscoelastic behavior in mature ligament. Although the origins of viscoelasticity in human ligament remain unresolved, our findings have helped narrow the possible contributions from extracellular matrix molecules. Future studies need to assess the inherent viscoelasticity of collagen by determining the influence of inter- and intramolecular collagen bonds, fluid flow, and fibril-associating collagens (i.e., type XII) on transient ligament behavior. The findings of this study progress the structure-function knowledge of ligament and are applicable to research seeking to engineer and evaluate replacement tissues.

GRANTS

Financial support from National Institute of Arthritis and Musculoskeletal and Skin Diseases Grant AR-047369 is gratefully acknowledged.

REFERENCES

- Al Jamal R, Roughley PJ, Ludwig MS. Effect of glycosaminoglycan degradation on lung tissue viscoelasticity. *Am J Physiol Lung Cell Mol Physiol* 280: L306–L315, 2001.
- Amiel D, Frank C, Harwood F, Fronck J, Akeson W. Tendons and ligaments: a morphological and biochemical comparison. *J Orthop Res* 1: 257–265, 1984.
- Bonifasi-Lista C, Lake SP, Small MS, Weiss JA. Viscoelastic properties of the human medial collateral ligament under longitudinal, transverse and shear loading. *J Orthop Res* 23: 67–76, 2005.
- Boorman RS, Norman T, Matsen FA 3rd, Clark JM. Using a freeze substitution fixation technique and histological crimp analysis for characterizing regions of strain in ligaments loaded *in situ*. *J Orthop Res* 24: 793–799, 2006.
- Bray DF, Frank CB, Bray RC. Cytochemical evidence for a proteoglycan-associated filamentous network in ligament extracellular matrix. *J Orthop Res* 8: 1–12, 1990.
- Butler SL, Kohles SS, Thielke RJ, Chen C, Vanderby R Jr. Interstitial fluid flow in tendons or ligaments: a porous medium finite element simulation. *Med Biol Eng Comput* 35: 742–746, 1997.
- Chahine NO, Chen FH, Hung CT, Ateshian GA. Direct measurement of osmotic pressure of glycosaminoglycan solutions by membrane osmometry at room temperature. *Biophys J* 89: 1543–1550, 2005.
- Chimich D, Shrive N, Frank C, Marchuk L, Bray R. Water content alters viscoelastic behaviour of the normal adolescent rabbit medial collateral ligament. *J Biomech* 25: 831–837, 1992.
- Ciarletta P, Micera S, Accoto D, Dario P. A novel microstructural approach in tendon viscoelastic modelling at the fibrillar level. *J Biomech* 39: 2034–2042, 2006.
- Davey KJ, Skegg DC. The effects of high concentrations of an electrolyte on the swelling of non-metabolizing tissue slices. *J Physiol* 212: 641–653, 1971.
- Elliott DM, Robinson PS, Gimbel JA, Sarver JJ, Abboud JA, Iozzo RV, Soslowsky LJ. Effect of altered matrix proteins on quasilinear viscoelastic properties in transgenic mouse tail tendons. *Ann Biomed Eng* 31: 599–605, 2003.
- Findley W, Lai J, Onaran K. *Creep and Relaxation of Nonlinear Viscoelastic Materials, with an Introduction to Linear Viscoelasticity*. Amsterdam: North Holland, 1976.
- Fung YC. *Biomechanics: Mechanical Properties of Living Tissues*. New York: Springer, 1993.
- Gandley RE, McLaughlin MK, Koob TJ, Little SA, McGuffee LJ. Contribution of chondroitin-dermatan sulfate-containing proteoglycans to the function of rat mesenteric arteries. *Am J Physiol Heart Circ Physiol* 273: H952–H960, 1997.
- Hansen KA, Weiss JA, Barton JK. Recruitment of tendon crimp with applied tensile strain. *J Biomech Eng* 124: 72–77, 2002.
- Hardingham TE, Muir H, Kwan MK, Lai WM, Mow VC. Viscoelastic properties of proteoglycan solutions with varying proportions present as aggregates. *J Orthop Res* 5: 36–46, 1987.
- Hascall VC, Riolo RL, Hayward J Jr, and Reynolds CC. Treatment of bovine nasal cartilage proteoglycan with chondroitinases from *Flavobacterium heparinum* and *Proteus vulgaris*. *J Biol Chem* 247: 4521–4528, 1972.
- Haut RC, Powlison AC. The effects of test environment and cyclic stretching on the failure properties of human patellar tendons. *J Orthop Res* 8: 532–540, 1990.
- Henninger HB, Maas SA, Underwood CJ, Whitaker RT, Weiss JA. Spatial distribution and orientation of dermatan sulfate in human medial collateral ligament. *J Struct Biol* 158: 33–45, 2007.
- Huang CY, Mow VC, Ateshian GA. The role of flow-independent viscoelasticity in the biphasic tensile and compressive responses of articular cartilage. *J Biomech Eng* 123: 410–417, 2001.
- Huang Y, Meek KM. Swelling studies on the cornea and sclera: the effects of pH and ionic strength. *Biophys J* 77: 1655–1665, 1999.
- Ilic MZ, Carter P, Tyndall A, Dudhia J, Handley CJ. Proteoglycans and catabolic products of proteoglycans present in ligament. *Biochem J* 385: 381–388, 2005.
- Koob TJ. Effects of chondroitinase-ABC on proteoglycans and swelling properties of fibrocartilage in bovine flexor tendon. *J Orthop Res* 7: 219–227, 1989.
- Koob TJ, Vogel KG. Site-related variations in glycosaminoglycan content and swelling properties of bovine flexor tendon. *J Orthop Res* 5: 414–424, 1987.
- Laasanen MS, Toyras J, Korhonen RK, Rieppo J, Saarakkala S, Nieminen MT, Hirvonen J, Jurvelin JS. Biomechanical properties of knee articular cartilage. *Biorheology* 40: 133–140, 2003.
- Lai WM, Hou JS, Mow VC. A triphasic theory for the swelling and deformation behaviors of articular cartilage. *J Biomech Eng* 113: 245–258, 1991.
- Lanir Y, Salant EL, Foux A. Physico-chemical and microstructural changes in collagen fiber bundles following stretch *in vitro*. *Biorheology* 25: 591–603, 1988.
- Liu X, Yeh ML, Lewis JL, Luo ZP. Direct measurement of the rupture force of single pair of decorin interactions. *Biochem Biophys Res Commun* 338: 1342–1345, 2005.
- Lujan TJ, Lake SP, Plaizier TA, Ellis BJ, Weiss JA. Simultaneous measurement of three-dimensional joint kinematics and ligament strains with optical methods. *J Biomech Eng* 127: 193–197, 2005.
- Lujan TJ, Underwood CJ, Henninger HB, Thompson BM, Weiss JA. Effect of dermatan sulfate glycosaminoglycans on the quasi-static material properties of the human medial collateral ligament. *J Orthop Res* 25: 894–903, 2007.
- Lujan TJ, Underwood CJ, Jacobs N, Weiss JA. Tissue swelling during extended material testing of ligaments (Abstract). *ASME Summer Bioengineering Conference*, Keystone Resort, CO, 2007.
- Matyas JR, Anton MG, Shrive NG, Frank CB. Stress governs tissue phenotype at the femoral insertion of the rabbit MCL. *J Biomech* 28: 147–157, 1995.
- Mijailovich SM, Stamenovic D, Brown R, Leith DE, Fredberg JJ. Dynamic moduli of rabbit lung tissue and pigeon ligamentum propatagiale undergoing uniaxial cyclic loading. *J Appl Physiol* 76: 773–782, 1994.
- Millesi H, Reihnsner R, Hamilton G, Mallinger R, Menzel EJ. Biomechanical properties of normal tendons, normal palmar aponeuroses, and tissues from patients with Dupuytren's disease subjected to elastase and chondroitinase treatment. *Clin Biomech (Bristol, Avon)* 10: 29–35, 1995.
- Moon DK, Woo SL, Takakura Y, Gabriel MT, Abramowitch SD. The effects of refreezing on the viscoelastic and tensile properties of ligaments. *J Biomech* 39: 1153–1157, 2006.

37. **Pioletti DP, Rakotomanana LR, Leyvraz PF.** Strain rate effect on the mechanical behavior of the anterior cruciate ligament-bone complex. *Med Eng Phys* 21: 95–100, 1999.
38. **Pogany G, Hernandez DJ, Vogel KG.** The in vitro interaction of proteoglycans with type I collagen is modulated by phosphate. *Arch Biochem Biophys* 313: 102–111, 1994.
39. **Provenzano PP, Heisey D, Hayashi K, Lakes R, Vanderby R Jr.** Subfailure damage in ligament: a structural and cellular evaluation. *J Appl Physiol* 92: 362–371, 2002.
40. **Puxkandl R, Zizak I, Paris O, Keckes J, Tesch W, Bernstorff S, Purslow P, Fratzl P.** Viscoelastic properties of collagen: synchrotron radiation investigations and structural model. *Philos Trans R Soc Lond B Biol Sci* 357: 191–197, 2002.
41. **Quapp KM, Weiss JA.** Material characterization of human medial collateral ligament. *J Biomech Eng* 120: 757–763, 1998.
42. **Raspanti M, Congiu T, Guizzardi S.** Structural aspects of the extracellular matrix of the tendon: an atomic force and scanning electron microscopy study. *Arch Histol Cytol* 65: 37–43, 2002.
43. **Raspanti M, Viola M, Sonaggers M, Tira ME, Tenni R.** Collagen fibril structure is affected by collagen concentration and decorin. *Biomacromolecules* 8: 2087–2091, 2007.
44. **Redaelli A, Vesentini S, Soncini M, Vena P, Mantero S, Montevecchi FM.** Possible role of decorin glycosaminoglycans in fibril to fibril force transfer in relative mature tendons—a computational study from molecular to microstructural level. *J Biomech* 36: 1555–1569, 2003.
45. **Robinson JR.** Control of water content of respiring kidney slices by sodium chloride and polyethylene glycol. *J Physiol* 282: 285–294, 1978.
47. **Robinson PS, Lin TW, Reynolds PR, Derwin KA, Iozzo RV, Soslowsky LJ.** Strain-rate sensitive mechanical properties of tendon fascicles from mice with genetically engineered alterations in collagen and decorin. *J Biomech Eng* 126: 252–257, 2004.
48. **Rubin MB, Bodner SR.** A three-dimensional nonlinear model for dissipative response of soft tissue. *Int J Solids Struct* 39: 5081–5099, 2002.
49. **Schmidt MB, Mow VC, Chun LE, Eyre DR.** Effects of proteoglycan extraction on the tensile behavior of articular cartilage. *J Orthop Res* 8: 353–363, 1990.
50. **Schuirman DJ.** A comparison of the two one-sided tests procedure and the power approach for assessing the equivalence of average bioavailability. *J Pharmacokinetic Biopharm* 15: 657–680, 1987.
51. **Scott JE.** Elasticity in extracellular matrix “shape modules” of tendon, cartilage, etc. A sliding proteoglycan-filament model. *J Physiol* 553: 335–343, 2003.
52. **Scott JE.** Proteodermatan and proteokeratan sulfate (decorin, lumican/fibromodulin) proteins are horseshoe shaped. Implications for their interactions with collagen. *Biochemistry* 35: 8795–8799, 1996.
53. **Scott JE, Thomlinson AM.** The structure of interfibrillar proteoglycan bridges (shape modules) in extracellular matrix of fibrous connective tissues and their stability in various chemical environments. *J Anat* 192: 391–405, 1998.
54. **Sun DD, Guo XE, Likhitanichkul M, Lai WM, Mow VC.** The influence of the fixed negative charges on mechanical and electrical behaviors of articular cartilage under unconfined compression. *J Biomech Eng* 126: 6–16, 2004.
55. **Sverdluk A, Lanir Y.** Time-dependent mechanical behavior of sheep digital tendons, including the effects of preconditioning. *J Biomech Eng* 124: 78–84, 2002.
56. **Thornton GM, Shrive NG, Frank CB.** Altering ligament water content affects ligament pre-stress and creep behaviour. *J Orthop Res* 19: 845–851, 2001.
57. **Tiderius CJ, Olsson LE, Nyquist F, Dahlberg L.** Cartilage glycosaminoglycan loss in the acute phase after an anterior cruciate ligament injury: delayed gadolinium-enhanced magnetic resonance imaging of cartilage and synovial fluid analysis. *Arthritis Rheum* 52: 120–127, 2005.
59. **Vogel KG, Paulsson M, Heinegard D.** Specific inhibition of type I and type II collagen fibrillogenesis by the small proteoglycan of tendon. *Biochem J* 223: 587–597, 1984.
60. **Woo SLY, Johnson GA, Smith BA.** Mathematical modeling of ligaments and tendons. *J Biomech Eng* 115: 468–473, 1993.
61. **Woo SLY, Orlando CA, Camp JT, Akeson WH.** Effects of postmortem storage by freezing on ligament tensile behavior. *J Biomech* 19: 399–404, 1986.
62. **Woo SL, Debski RE, Withrow JD, Jansushek MA.** Biomechanics of knee ligaments. *Am J Sports Med* 27: 533–543, 1999.
63. **Yamagata T, Saito H, Habuchi O, Suzuki S.** Purification and properties of bacterial chondroitinases and chondrosulfatases. *J Biol Chem* 243: 1523–1535, 1968.
64. **Zhu W, Mow VC, Koob TJ, Eyre DR.** Viscoelastic shear properties of articular cartilage and the effects of glycosidase treatments. *J Orthop Res* 11: 771–781, 1993.